Millimeter-Wave Radar Sensing of Airborne Chemicals

Nachappa (Sami) Gopalsami, *Senior Member, IEEE*, and Apostolos (Paul) C. Raptis, *Member, IEEE*

***Abstract*—This paper discusses the development of a millimeter-wave radar chemical sensor for applications in environmental monitoring and arms-control treaty verification. The purpose of this paper is to investigate the use of fingerprint-type molecular rotational signatures in the millimeter-wave spectrum to sense airborne chemicals. The millimeter-wave sensor, operating in the frequency range of 225–315 GHz, can work under all weather conditions and in smoky and dusty environments. The basic configuration of the millimeter-wave sensor is a monostatic swept-frequency radar that consists of a millimeter-wave sweeper, a hot-electron bolometer or Schottky barrier detector, and a corner-cube reflector. The chemical plume to be detected is situated between the transmitter/detector and reflector. Millimeter-wave absorption spectra of chemicals in the plume are determined by measuring the swept-frequency radar return signals with and without the plume in the beam path. The problem of pressure broadening, which hampered open-path spectroscopy in the past, has been mitigated in this paper by designing a fast sweeping source over a broad frequency range. The heart of the system is a backward-wave oscillator (BWO) tube that can be tuned over 220–350 GHz. Using the BWO tube, we built a millimeter-wave radar system and field-tested it at the Department of Energy Nevada Test Site, Frenchman Flat, near Mercury, NV, at a standoff distance of 60 m. The millimeter-wave system detected chemical plumes very well; detection sensitivity for polar molecules such as methylchloride was down to 12 ppm for a 4-m two-way pathlength.**

***Index Terms*—Airborne chemicals, backward-wave oscillators, millimeter waves, remote sensing, rotational spectroscopy.**

I. Introduction

REMOTE OR standoff detection of airborne chemicals is gaining importance for arms-control treaty verification and environmental monitoring. When compared with point detection or sampling techniques, the remote method is nonintrusive and can be used to monitor wide areas. Optical and laser remote techniques are under active development in the infrared, visible, and ultraviolet regions of the electromagnetic spectrum [1]–[3]. Although quite sensitive to volatile organic and other hazardous chemicals, these systems are susceptible to weather conditions and are too complex for field use. The purpose of this paper is to investigate the use of the millimeter-wave spectrum for remote detection of chemicals. Since millimeter-wave sensors use longer wavelengths than those of optics, they can operate under all weather conditions and in smoky and dusty environments.

Millimeter-wave spectroscopy is a well-established laboratory technique for determining the structure and dynamics of molecules in the gas or vapor phase [4]. Millimeter-wave spectral lines are narrow and nearly 100% specific when analyzed in a gas cell under low pressures (< 1 torr). However, when applied to open-air monitoring, the spectral lines become broad because of molecular collisions that occur at high (i.e., atmospheric) pressure. A typical air-broadening parameter of a molecule is 4 MHz/torr in half-width at half-height (HWHT) and $\approx$4 GHz at 1 atm. Conventional detection methods that are capable of high detection sensitivities at low pressures, e.g., Stark modulation or phase-locked techniques, are not directly applicable to open-air detection. Hence, new detection methods and systems are needed for remote detection of trace chemicals in air.

One way to overcome the pressure-broadening effect is to use a swept-frequency millimeter-wave source that can sweep over a broad frequency range in a short time. The wide-frequency sweep improves spectral line resolution and molecular selectivity, whereas the fast sweep allows for efficient baseline subtraction by direct video detection. The feasibility of open-air millimeter-wave spectroscopy was first demonstrated with a monostatic swept-frequency radar system in the 225–315-GHz range [5]. The millimeter waves were generated with a low-frequency sweeper and low-power frequency triplers. The narrow bandwidth of the triplers also limited the tuning range to within 50 GHz. The proof-of-principle of this system was tested by detecting D_2O in open air. In addition, the chemical selectivity of the technique was demonstrated by a special deconvolution procedure [6]. Individual chemicals in a multicomponent mixture were determined from both simulated and experimental spectra.

With recently available backward-wave oscillator (BWO) tubes [7], we developed a prototype radar system that can sweep the entire frequency range within 10 ms and generate up to 30 mW of power [8]. This greater power allows a longer detection range and the wider tuning range improves the resolution of spectral lines. The radar system was field-tested at the Department of Energy (DOE) Nevada Test Site, Frenchman Flat, near Mercury, NV, at a standoff distance of 60 m. Two chemicals, i.e., methylchloride and butanol, were released from a wind tunnel in different concentrations. In terms of millimeter-wave spectral properties, these chemical represent two distinct classes: methylchloride has distinct broad spectral lines, while butanol has monotonically increasing continuum absorption with respect to frequency. This paper describes the

Manuscript received July 20, 1999; revised August 16, 2000. This work was supported by the U.S. Department of Energy, Office of Nonproliferation and National Security, Office of Research and Development under Contract W-31-109-ENG-38.

The authors are with the Energy Technology Division, Argonne National Laboratory, Argonne, IL 60439 USA.

Publisher Item Identifier S 0018-9480(01)02419-X.

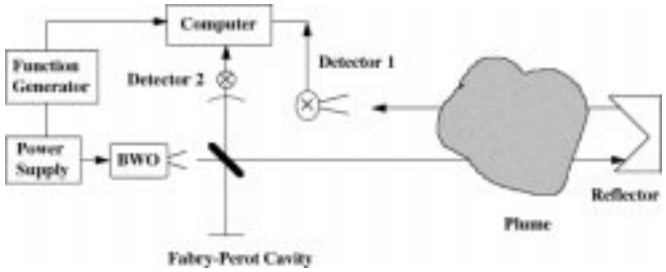

Fig. 1. Schematic diagram of millimeter-wave radar system.

millimeter-wave sensor, field test setup, and test results from methylchloride and butanol releases.

II. Description of Millimeter-Wave Radar Sensor

The millimeter-wave sensor, shown in Fig. 1, is a monostatic radar system that operates in an atmospheric window in the frequency range of 225–315 GHz. Swept-frequency signals in this range are generated and transmitted through a chemical plume via a lens antenna. A corner cube, located behind the plume, returns the radar signals through the plume to a millimeter-wave detector that is next to the transmitter. Millimeter-wave absorption spectra of chemicals in the plume are determined by measuring swept-frequency radar signals with and without the plume in the beam path. A Fabry–Perot (F–P) cavity, which consumes a small part of the millimeter-wave energy, generates frequency markers for on-the-fly calibration of frequencies. The F–P cavity markers allow better subtraction of baseline and signal averaging.

The millimeter-wave sweeper was built with an OB-30 BWO tube [9], which structurally consists of an electron emission source (cathode) and a slow-wave structure (anode) housed in a vacuum envelope, 25 mm in diameter and 35 mm in length. Coherent radiation is produced when electrons emitted by the cathode are accelerated over the slow-wave structure; the frequency of oscillation is determined by the electron velocity and the period of the slow-wave structure. A permanent magnet made of cobalt–samarium alloy produces a dc magnetic field (≈7000 G) to steer the electron beam over the slow-wave structure. The millimeter-wave radiation generated in the tube (with a power $\approx$ 10 mW) is coupled to a scalar horn through an overmoded rectangular waveguide attached to the tube structure. Oscillation frequency varies in a nonlinear fashion with the electrical potential between the cathode and anode; it is tunable between 220–350 GHz, corresponding to a voltage range of 1000–3700 V. Due to its large tuning slope (e.g., 75 MHz/V at 2400 V), a small ripple or fluctuation in the high-voltage power supply will alter the tube frequency considerably (e.g., a 10-mV fluctuation produces a 0.75-MHz variation). The need for fast sweeping of high voltage over a range of 1000–4000 V with a low ripple content makes the power supply requirements stringent for spectroscopic application. A high-voltage power supply, capable of sweeping from 1000 to 4000 V in ≈ 1 ms with less than 2 mV of ripple, was designed and built in collaboration with The Ohio State University, Columbus [10].

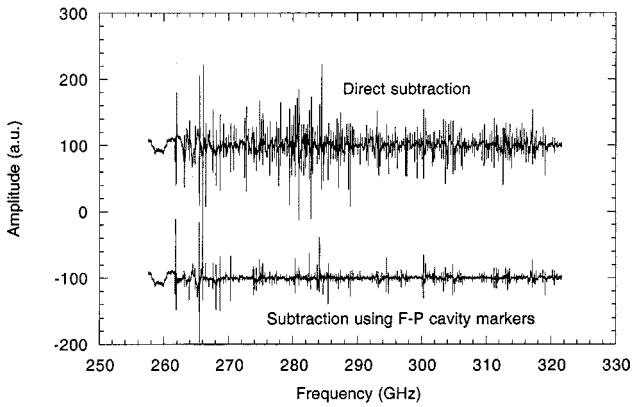

Fig. 2. Effect of using F–P cavity scheme in baseline subtraction; frequency swept from 257.6 to 321.6 GHz in 1 s.

Yet, with free-running oscillators, it is nearly impossible to achieve the long-term frequency stability required for baseline subtraction and signal averaging because inherent frequency drifts are caused by power supply noise and thermal instability of the tube structure. Hence, in high-resolution spectroscopy, one often resorts to phase-locked control of the BWO, but this is rather slow for the wide-frequency sweep that is required in open-path spectroscopy. In this paper, we use a quasi-optical F–P cavity for on-the-fly calibration of frequencies [11]. When swept-frequency radiation is applied to the cavity, resonant peaks are generated each time the cavity spacing is equal to the integral number of half-wavelengths. For a cavity length of $d = 53$ cm that we used, the marker spacing in frequency is given by $c/2d = 282.83$ MHz, where c is the wave velocity in free space. Data that correspond to radar signal and cavity markers are collected during each sweep. Since the cavity markers correspond to actual frequencies during a sweep, the cavity markers and corresponding samples of radar data are aligned with respect to an initial set of cavity markers by a MATLAB-based frequency calibration software that we have built. The radar data between the cavity markers are interpolated linearly. Fig. 2 shows, for instance, subtraction of two swept-frequency traces, with and without the use of cavity markers. In practice, the amplitude of the cavity peaks varies widely from peak to peak, some appearing below the noise threshold. In the frequency calibration software, only those cavity peaks that are above a certain threshold are used for marker alignment. In those instances where the cavity markers are absent, the baseline correction has not been effective. Further improvement is possible with a longer cavity because of narrower frequency spacing between the markers.

III. Field Test Setup

The millimeter-wave system was field-tested at the Nevada Test Site, Frenchman Flat, near Mercury, NV. A wind tunnel, capable of producing well-characterized chemical plumes of 2-m diameter at the exit point, was used to release desired concentrations of airborne chemicals. Testing of the millimeter-wave sensor was conducted in a trailer 60 m from the wind tunnel

Fig. 3. Millimeter-wave-system trailer, wind tunnel, and corner cube.

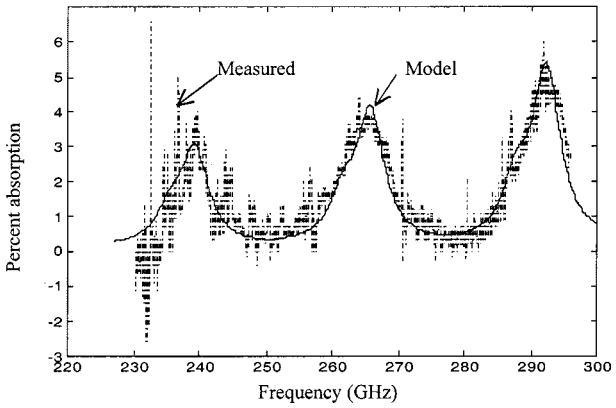

Fig. 4. Model and measured methylchloride spectra obtained in laboratory from 377 mtorr of methylchloride mixed with nitrogen to 1 atm in 1.4-m gas cell.

in the cross-wind direction. Fig. 3 shows the millimeter-wave sensor trailer together with the wind tunnel and corner cube. The millimeter-wave radiation was transmitted through a trailer window into the wind-tunnel plume. The window was covered with a plastic film that was transparent to millimeter waves. A 6-in lens, focused at infinity, provided a highly directed beam. The cone angle of the beam was 0.37° with a footprint of 0.6 m at the wind tunnel. An aluminum corner cube with a 0.9 × 0.9 × 0.9 m opening was mounted behind the plume to return radar signals. The return signals were collected by a 6-in lens coupled to a liquid-helium-cooled (hot-electron) bolometer detector situated next to the transmitter. For safety, the trailer was not occupied during the release, leaving the millimeter-wave sensor unattended during the test. Data were collected remotely from the wind-tunnel control room 1.7 km away, via an RF link between a master computer in the control room and the data-acquisition (slave) computer in the trailer. Meteorological conditions during the tests were relatively benign: 35 °C, 8% relative humidity, and winds of 5–10 m/s.

IV. Test Results

The millimeter-wave spectral data of methylchloride and butanol were first measured in the laboratory with a 1.4-m gas cell. To simulate atmospheric pressure, a quantity of each chemical was mixed with nitrogen to a pressure of 1 atm. Fig. 4 shows

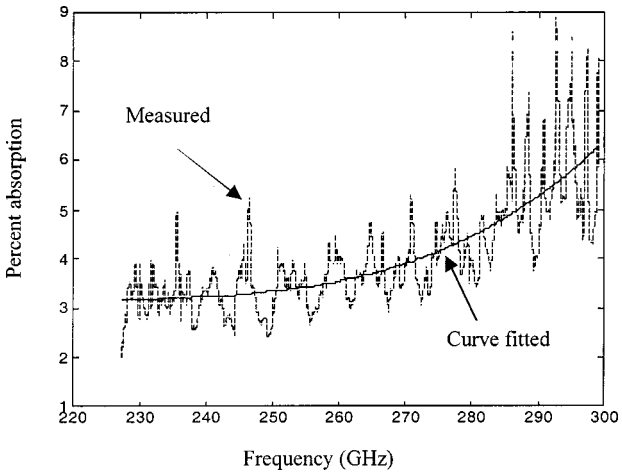

Fig. 5. Butanol spectrum obtained in laboratory from 664 mtorr of butanol mixed with nitrogen to 1 atm in 1.4-m gas cell.

the measured absorption spectra of 377 mtorr of methylchloride in nitrogen in the frequency range of 230–298 GHz. The noise-like fluctuations in the data is due to inadequate baseline subtraction in spite of employing the F–P cavity technique. Furthermore, the percent absorption values were calculated by dividing the difference signal with the reference signal, i.e., $100(1 - P_2(t)/P_1(t))$, where $P_2(t)$ and $P_1(t)$ correspond to the data with and without the gas in the cell. Since the reference signal varies widely in amplitude, the division operation amplifies the error in baseline subtraction, especially when $P_1(t)$ is close to zero. In principle, these fluctuations can be completely subtracted out with a longer F–P cavity and better interpolation software. For the purpose of measuring broad atmospheric-pressure lines, however, the measured data can be smoothed out by fitting a model-based absorption spectrum, as shown by the solid line in Fig. 4. The model spectral lines were simulated with a Lorentzian line-shape function using data from the Jet Propulsion Laboratory (JPL), Pasadena, CA, molecular data base [12].

Fig. 5 shows the measured absorption spectrum of butanol obtained in the laboratory from 664 mtorr of butanol mixed with nitrogen to 1 atm. Unlike with methylchloride, millimeter-wave absorption of butanol appears to be a continuum and it increases with frequency. The fluctuations in the measured spectra result from baseline variation due to change in signal power with frequency, and they match exactly those of the reference signal; hence, they are not part of the butanol absorption lines. Since butanol is not included in any known databases, we fitted a polynomial curve to smooth out the measured data and used it as the model spectrum of butanol for later data analysis.

Before the tests, using acetonitrile in a gas cell, we calibrated the system frequencies. A triangular ramp with a 40-ms period was used to sweep from 226 to 298 GHz, and data were collected during the up-ramp. Each chemical was released in an on–off pattern, each pattern typically lasting ≈ 5 min. Reference and plume signals were collected during the plume-off and plume-on periods, respectively. Methylchloride data were collected as an average of 100 sweeps, whereas butanol data were collected sequentially (without averaging) before and during release. To cover the sensor's detection range, we released methylchloride in concentrations from 5 to 500 ppm.

Butanol was released only at high concentrations from 410 to 1200 ppm. Three channels of data were collected: dc- and ac-coupled data from the bolometer and the F–P cavity. While the ac-coupled channel worked well, the dc-coupled channel drifted over time and saturated the detector preamplifier. To interpret the spectral data, we will next develop data analysis procedures for the dc- and ac-coupled cases.

A. DC-Coupled Data

The dc-coupled detector signal is proportional to the absolute power of millimeter waves with respect to frequency. Let $P_0(t)$ be the output signal of the transmitter as a function of sweep time, and $P_1(t)$ and $P_2(t)$ be the detector signals without and with the plume, called reference and plume signals, respectively. Note that sweep time t has a one-to-one correspondence with millimeter-wave frequency v. While the millimeter-wave frequency is in the hundreds of gigahertz range, the bandwidth of the detector signal is generally less than 1 MHz. Then

$$P_1(t) = P_0(t)T \tag{1}$$

and

$$P_2(t) = P_0(t)T\exp\big[-\alpha(t)C\ell\big] \tag{2}$$

where T is the two-way transmission coefficient of the atmosphere between the transmitter antenna and receiver, $\alpha(t)$ is the absorption coefficient (cm^{-1} of 1 ppm of chemical in the air at sweep time t corresponding to millimeter-wave frequency v, C is the concentration of the chemical (parts per million), and ℓ is the path length (centimeters) of the plume ($\ell = 400$ cm in our case). The difference between the reference and plume signals $D(t)$ is given by

$$D(t) = P_1(t) - P_2(t) = P_1(t)\Big\{1 - \exp\big[-\alpha(t)C\ell\big]\Big\}. \tag{3}$$

Thus, in the dc-coupled case, the absorption coefficient $\alpha(t)$ can be determined by dividing (3) by the reference signal $P_1(t)$. For trace amounts of gases to be released in the open air, $\alpha(t)C\ell$ is small and (3) becomes

$$D(t) \cong \alpha(t)C\ell P_1(t). \tag{4}$$

B. AC-Coupled Data

During collection of ac-coupled data, the dc-level signal is blocked, and only the ac-type signal is collected from the detector circuit. This mode of data collection avoids saturation of the detector preamplifier when the dc signal drifts with time. Let a bar over the variables represent ac-coupled signal operation. For the ac-coupled case, (1) and (2) become

$$\bar{P}_1(t) = \bar{P}_0(t)T \tag{5}$$

and

$$\bar{P}_2(t) = \bar{P}_0(t)T - \overline{P_0(t)T\alpha(t)C\ell} + \frac{\overline{P_0(t)T[\alpha(t)C\ell]^2}}{2} - \cdots. \tag{6}$$

The difference between the reference and plume signals, i.e., (5) − (6), becomes

$$\bar{D}(t) = \bar{P}_1(t) - \bar{P}_2(t) \cong \overline{P_0(t)\alpha(t)}C\ell T. \tag{7}$$

Unlike with the dc-coupled signal of (3), it is not possible to separate out the absorption coefficient because $P_1(t)$ is not available in the ac-coupled case. Let $P_0(t)$ be represented as an ac signal superimposed on a dc signal

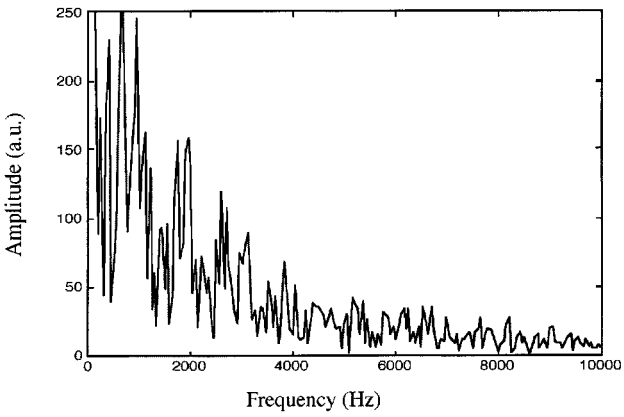

Fig. 6. Absolute value of Fourier transform of reference signal collected with a 3-kHz low-pass filter; the signal bandwidth is proportional to the sweep range and how fast the BWO signal fluctuations inherent in the frequency range are swept in time.

$$P_0(t) = P_{0,\mathrm{DC}} + P_{0,\mathrm{AC}}(t). \tag{8}$$

Then

$$\bar{D}(t) = \overline{P_0(t)\alpha(t)}C\ell T = P_{0,\mathrm{DC}}\alpha(t)C\ell T + \overline{P_1(t)\alpha(t)}C\ell. \tag{9}$$

Thus, the difference signal $\bar{D}(t)$ is the sum of the plume absorption coefficient (times a constant) and ac part of the amplitude modulation of the reference signal by the plume absorption coefficient. Since $\alpha(t)$ is broad due to pressure broadening, its frequency content is low. On the other hand, the reference signal that acts as a carrier has a high-frequency content (see Fig. 6 for a typical test reference signal). Since in the Fourier transformation of the amplitude-modulated signal, frequencies will be centered on the carrier (reference signal) frequency, a high-pass filter with passband frequencies above that of $\alpha(t)$ will pass only the amplitude-modulated part of the signal in (9). Letting the superscript $\sim$ represent high-pass filtered signal

$$\tilde{D}(t) = \tilde{P}_1(t) - \tilde{P}_2(t) \cong \tilde{P}_1(t)\alpha(t)C\ell. \tag{10}$$

To illustrate the modulation and filtering effect, let us choose for $\bar{P}_1(t)$ one of the ac-coupled reference signals collected in the tests. We will arbitrarily add a dc value to simulate $P_1(t)$ because it is related to transmitter power, which must be a positive signal. The plume signal $P_2(t)$ is obtained by multiplication with an absorption coefficient function related to molecular absorption. Let us choose two types of absorption coefficients to simulate methylchloride- and butanol-like absorption

$$\alpha(t) = \frac{0.01(\Delta t)^2}{(t-t_0)^2+(\Delta t)^2}$$
to simulate methylchloride absorption (11)

and

$$\alpha(t) = \alpha_0 + kt^2 \quad \text{to simulate butanol absorption.} \tag{12}$$

In (11) and (12), t is sweep time from 0 to 0.02 s, $\Delta t = 0.002$ s, and $t_0 = 0.01$ s, and α_0 and k are constants. The absorption line in (11) is centered at 0.01 s with its HWHT width covering 10% of the total sweep time. Considering the relative bandwidths of measured signals with those of molecular

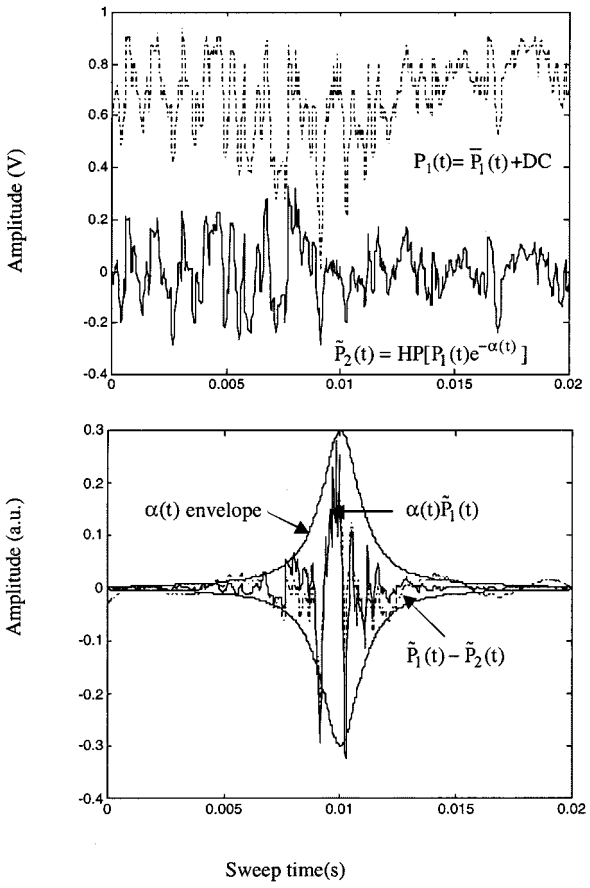

Fig. 7. Simulated data showing modulation and filtering effects for distinct absorption line.

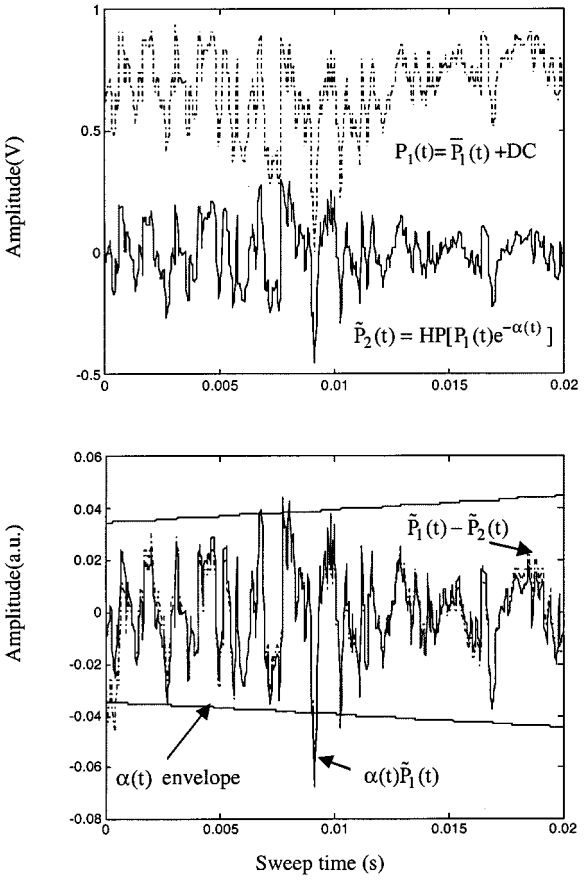

Fig. 8. Simulated data showing modulation and filtering effects for continuum absorption.

spectral lines, we chose a 200-Hz high-pass elliptic filter to obtain signals in (10). For example, $P_1(t)$ and $P_2(t)$ were filtered with a 200-Hz high-pass filter to obtain $\tilde{P}_1(t)$ and $\tilde{P}_2(t)$. For the two cases of $\alpha(t)$ in (11) and (12), Figs. 7 and 8, respectively, present the sequence of operations carried out on the reference signal. Shown in the figures are the signal $P_1(t)$, filtered signal $\tilde{P}_2(t)$, the difference signal $\tilde{P}_1(t) - \tilde{P}_2(t)$, modulated signal $\alpha(t)\tilde{P}_1(t)$, and an arbitrarily scaled $\alpha(t)$ envelope. The difference signal and absorption-coefficient-modulated reference signal agree well in both of the examples, as predicted by (10). Note that the difference signal follows the modulation envelope of $\alpha(t)$ and that the actual peaks and valleys under the envelope are representative of the reference signal at the corresponding time instants.

These examples show that the concentration of a chemical can be quantified by model-fitting the absorption-coefficient-modulated reference signal $\alpha_m(t)\tilde{P}_1(t)$ to the difference signal $\tilde{P}_1(t) - \tilde{P}_2(t)$, where $\alpha_m(t)$ is the model absorption line for 1 ppm of the chemical that can be determined either from one of the published molecular data bases, such as the JPL catalog, or by measuring it with a gas-cell spectrometer. That is, $\tilde{D}(t)$ in (10) can be fitted with a model-based signal $\tilde{E}(t)$, given by

$$\tilde{E}(t) = \alpha_m(t)\hat{C}\ell\tilde{P}_1(t) \tag{13}$$

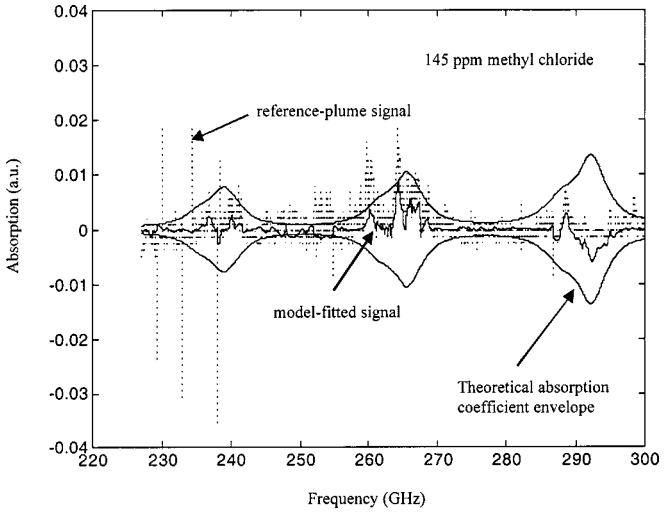

Fig. 9. Difference signal between reference and plume, model-fitted signal, and absorption coefficient envelope for 145-ppm methylchloride.

where $\hat{C}$ is an estimate of concentration C and may be chosen so that it minimizes the values of the integral of the squared error $S(\hat{C})$ over the sweep time between 0 and t_1. Thus,

$$S(\hat{C}) = \int_0^{t_1} \left[\alpha_m(t)\hat{C}\ell\tilde{P}_1(t) - \tilde{P}_1(t) + \tilde{P}_2(t)\right]^2 dt. \tag{14}$$

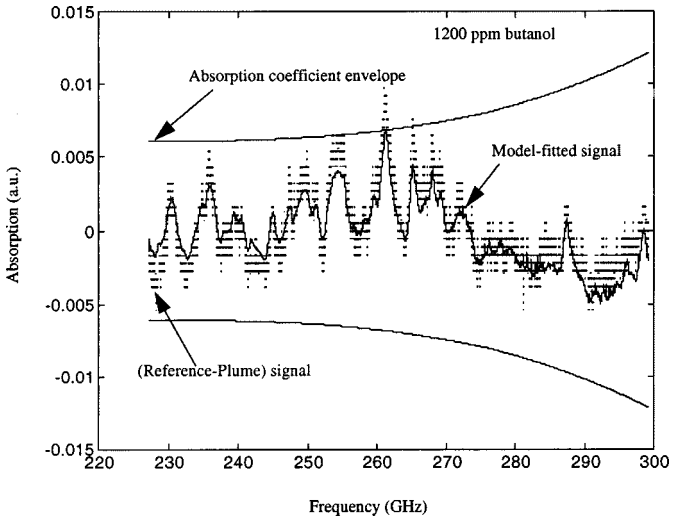

Fig. 10. Difference signal between reference and plume, model-fitted signal, and absorption coefficient envelope for 1200-ppm butanol.

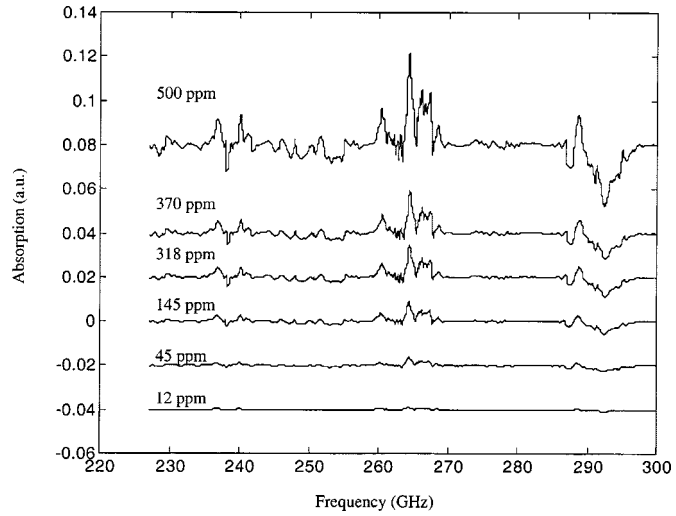

Fig. 11. Model-fitted signals for various concentrations of methylchloride.

By setting $dS(\hat{C})/d\hat{C} = 0$, optimal estimate $\hat{C}_{\rm opt}$ can be determined by

$$\hat{C}_{\rm opt} = \frac{\int_0^{t_1} \alpha_m(t)\ell\tilde{P}_1(t)\left[\tilde{P}_1(t) - \tilde{P}_2(t)\right]dt}{\int_0^t \left[\alpha_m(t)\ell\tilde{P}_1(t)\right]^2 dt}. \qquad (15)$$

The model-based analysis is applied in Fig. 9 by using ac-coupled data of 145-ppm methylchloride. The figure presents the difference signal between the reference and plume and model-fitted signal. The model fits the measured data well; thus, it eliminates the high-frequency noise. To show that the difference signal is an amplitude modulation of the reference signal by the plume absorption coefficient, we have overlain an envelope of arbitrarily scaled model absorption curves. Fig. 10 presents the corresponding analysis for buatnol using ac-coupled data of 1200-ppm butanol.

Figs. 11 and 12 present plots of the model-fitted data for methylchloride and butanol, respectively, for various concentrations. The corresponding values of $\hat{C}_{\rm opt}$, from (15), are plotted

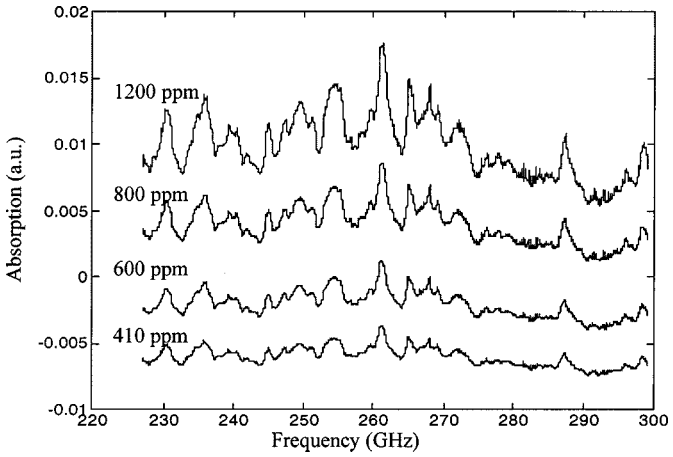

Fig. 12. Model-fitted signals for various concentrations of butanol.

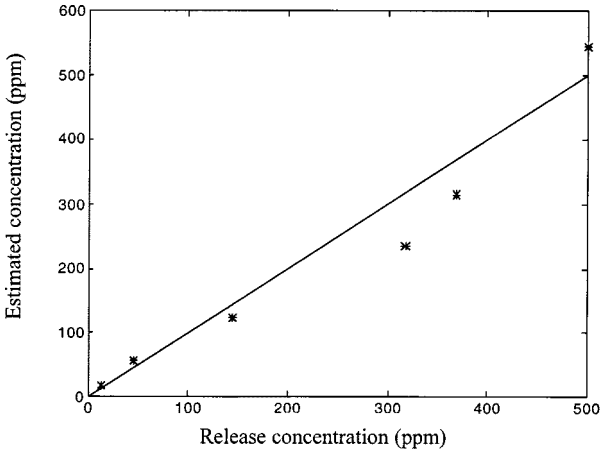

Fig. 13. Estimated versus release concentration of methylchloride (based on model fit).

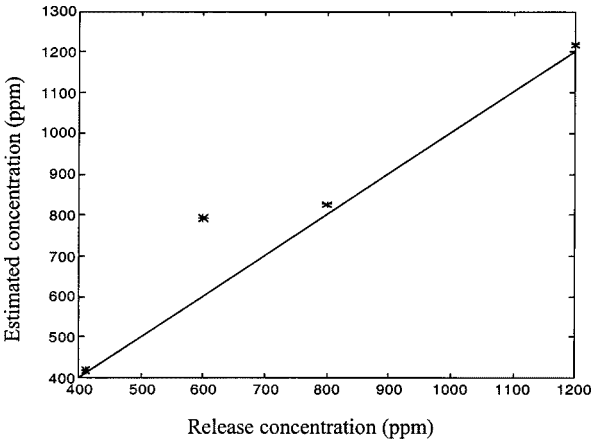

Fig. 14. Estimated versus release concentration of butanol (based on model fit).

in Figs. 13 and 14, respectively, with respect to the actual release concentrations. The value of $\hat{C}_{\rm opt}$ calculated from the model

provides a good estimate of the release concentration. The deviation of measured data, in some cases from the linear fit, may be attributed to signal fluctuations due to frequent wind gusts that were laden with sand particles. This is particularly noticeable with butanol for which data were not averaged.

V. Conclusions

A millimeter-wave radar chemical sensor was developed and field tested at the Nevada Test Site. The objective of the test was to demonstrate the capability of the sensor to remotely detect chemicals that are pertinent to verification of the arms-control treaty and environmental monitoring. The test of the sensor was conducted in a trailer at a standoff distance of 60 m from a 2-m-diameter plume. The return of radar signals was provided by a 0.9-m corner cube mounted behind the plume.

Although both dc- and ac-coupled data were collected remotely from a control room, the dc-coupled signals drifted between the time when the reference and plume signals were collected, and eventually saturated the detector preamplifier. Due to the dc drift, we could not absolutely determine molecular absorption with conventional procedures. The ac-coupled mode of data collection, on the other hand, worked well during the entire test period of ≈ 7 h. However, the interpretation of ac-coupled data is not straightforward, particularly for broad absorption lines occurring at atmospheric pressure.

A new model-based analysis procedure has been developed to interpret and quantify the acquired ac-coupled data. The analysis shows that the difference between the reference and plume signals for the ac-coupled (high-pass filtered) case is essentially an amplitude modulation of the reference signal by the plume absorption function. The correlation constant between the measured and model data provides a quantitative estimate of the chemical concentration. Good agreement between the measured and model data was obtained for various release concentrations of methylchloride and butanol. A linear fit was obtained between the estimated and actual concentrations. The detection sensitivity of the sensor, for example, was 12 ppm for methylchloride over a 4-m pathlength.

Since the long-term stability of the millimeter-wave sweeper is generally poor, it was necessary to keep the time interval between the reference and plume signals short (within 2–3 min) to obtain reproducible results. One approach to further improve detection sensitivity is to use two reflectors, one in front and another in back of the plume, and to steer the millimeter-wave beam between the two reflectors. This allows for long signal averages, while the time interval between the collection of reference and plume signals remains short.

Acknowledgment

The authors thank R. N. Lanham, Argonne National Laboratory, Argonne, IL, and E. R. Koehl, Argonne National Laboratory, Argonne, IL, for their help with the field test, and D. Morgan, Argonne National Laboratory, Argonne, IL, and T. Elmer III, Argonne National Laboratory, Argonne, IL, for help with the data analysis.

References

[1] W. B. Grant, R. H. Kagann, and W. A. McClenny, "Optical remote measurement of toxic gases," *J. Air Waste Manag. Assoc.*, vol. 42, pp. 18–30, 1992.

[2] S. P. Levine and G. M. Russwurm, "Fourier transform infrared optical remote sensing for monitoring airborne gas and vapor contaminants in the field," *Trends Analyt. Chem.*, vol. 13, pp. 258–262, 1994.

[3] J. V. Cernius, D. A. Elser, and J. Fox, "Remote active spectrometer," *SPIE Laser Applicat. Metrol., Earth, Atmospher. Remote Sensing*, vol. 1062, pp. 164–171, 1989.

[4] W. Gordy and R. L. Cook, *Microwave Molecular Spectra*. New York: Wiley, 1984.

[5] N. Gopalsami, S. Bakhtiari, A. C. Raptis, S. L. Dieckman, and F. C. D. Lucia, "Millimeter-wave measurements of molecular spectra with application to environmental monitoring," *IEEE Trans. Instrum. Meas.*, vol. 45, pp. 225–230, Feb. 1996.

[6] N. Gopalsami, S. Bakhtiari, A. C. Raptis, and S. L. Dieckman, "Millimeter-wave sensor for monitoring effluents," U.S. Patent 5 468 964, Nov. 1995.

[7] M. B. Golant, Z. T. Alekseenko, Z. S. Korotkova, L. A. Lunkina, A. A. Negirev, O. P. Petrova, T. B. Rebrova, and V. S. Savelev, *Prib. Tekh. Eksp.*, vol. 3, p. 231, 1969.

[8] N. Gopalsami, S. Bakhtiari, and A. C. Raptis, "Open-path millimeter-wave spectroscopy in the 225–315 GHz range," in *Proc. SPIE Int. Millimeter and Submillimeter Waves Applicat. III Conf.*, vol. 2842, 1996, pp. 274–283.

[9] *Technical Manual*, Istok Res. Prod. Corporation, Fryazino, Russia, 1994.

[10] D. T. Petkie, T. M. Goyette, R. Bettens, S. P. Belov, S. Albert, P. Helminger, and F. C. De Lucia, "A fast-scan submillimeter spectroscopic technique," *Rev. Sci. Instrum.*, vol. 68, pp. 1675–1683, 1997.

[11] A. Dryagin, V. V. Parshin, A. F. Krupnov, N. Gopalsami, and A. C. Raptis, "Precision broadband wavemeter for millimeter and submillimeter range," *IEEE Trans. Microwave Theory Tech.*, vol. 44, pp. 1610–1613, Sept. 1996.

[12] R. L. Poynter and H. M. Pickett, *Submillimeter, Millimeter, and Microwave Spectral Line Catalog*. Pasadena, CA: Jet Propulsion Lab., 1983, vol. 80-23.

Nachappa (Sami) Gopalsami (S'77–M'79–SM'95) received the B.E. and M.S. degrees in electrical engineering from the University of Madras, Madras, India, in 1970 and 1973, respectively, and the Ph.D. degree in electrical engineering and computer science from the University of Illinois at Chicago in 1981.

In 1980, he joined the Argonne National Laboratory, Argonne, IL, where he is currently an Electrical Engineer in the Sensor, Instrumentation and Nondestructive Evaluation (NDE) Section, Energy Technology Division. His current research interests are in the application of microwaves and millimeter waves for sensors and NDE. He has authored or co-authored over 75 technical papers in the area of sensors and NDE and holds four U.S. patents.

Dr. Gopalsami is a member of Sigma Xi. He was the recipient of a 1996 *Research and Development Magazine* Research and Development 100 Award for the development of millimeter-wave fabric inspection system. He was also the recipient of the 1995 Outstanding Paper Award presented by the American Society of Nondestructive Testing for his paper entitled "Millimeter-Wave Imaging for Nondestructive Evaluation of Materials," which was published in *Materials Evaluation.*

Apostolos (Paul) C. Raptis (S'66–M'67) received the B.E. degree from the University of Detroit, Detroit, MI, in 1965, the M.S. degree in electrical engineering from the University of Iowa, Iowa City, in 1967, and the Ph.D. degree in electrical engineering for the University of Akron, Akron, OH, in 1973.

From 1967 to 1969, he was with the Gulf Research and Development Center, Pittsburgh, PA. In 1974, he joined the Argonne National Laboratory, Argonne, IL, where he is currently a Senior Electrical Engineer and Section Manager for the Sensor, Instrumentation and Nondestructive Evaluation (I&NDE) Section, Energy Technology Division. He has authored or co-authored over 150 publications in the areas of I&NDE.

Dr. Raptis is a member of Sigma Tau, Eta Kappa Nu, and Sigma Xi. He has been a member of numerous advisory committees for the Department of Energy. He was the recipient of a 1996 *Research and Development Magazine* Research and Development 100 Award for the development of a millimeter-wave fabric inspection system. He was also the recipient of the 1995 Outstanding Paper Award presented by the American Society of Nondestructive Testing for his paper entitled, "Millimeter-Wave Imaging for Nondestructive Evaluation of Materials," which was published in *Materials Evaluation*.